Contrib Mineral Petrol
DOI 10.1007/s00410-007-0239-z

ORIGINAL PAPER

Seawater-like trace element signatures (REE + Y) of Eoarchaean chemical sedimentary rocks from southern West Greenland, and their corruption during high-grade metamorphism

C. R. L. Friend · A. P. Nutman · V. C. Bennett · M. D. Norman

Received: 10 July 2006 / Accepted: 11 July 2007

Abstract Modern chemical sediments display a distinctive rare earth element + yttrium (REE + Y) pattern involving depleted LREE, positive La/La*$_{SN}$, Eu/Eu*$_{SN}$, and Y_{SN} anomalies (SN = shale normalised) that is related to precipitation from circumneutral to high pH waters with solution complexation of the REEs dominated by carbonate ions. This is often interpreted as reflecting precipitation from surface waters (usually marine). The oldest broadly accepted chemical sediments are c. 3,700 Ma amphibolite facies banded iron-formation (BIF) units in the Isua supracrustal belt, Greenland. Isua BIFs, including the BIF international reference material IF-G are generally considered to be seawater precipitates, and display these REE + Y patterns (Bolhar et al. in Earth Planet Sci Lett 222:43–60, 2004). Greenland Eoarchaean BIF metamorphosed up to granulite facies from several localities in the vicinity of Akilia (island), display REE + Y patterns identical to Isua BIF, consistent with an origin by chemical sedimentation from seawater and a paucity of clastic input. Furthermore, the much-debated magnetite-bearing siliceous unit of "earliest life" rocks (sample G91/26) from Akilia has the same REE + Y pattern. This suggests that sample G91/26 is also a chemical sediment, contrary to previous assertions (Bolhar et al. in Earth Planet Sci Lett 222:43–60, 2004), and including suggestions that the Akilia unit containing G91/26 consists entirely of silica-penetrated, metasomatised, mafic rock (Fedo and Whitehouse 2002a). Integration of our trace element data with those of Bolhar et al. (Earth Planet Sci Lett 222:43–60, 2004) demonstrates that Eoarchaean siliceous rocks in Greenland, with ages from 3.6 to 3.85 Ga, have diverse trace element signatures. There are now geographically-dispersed, widespread examples with Isua BIF-like REE + Y signatures, that are interpreted as chemically unaltered, albeit metamorphosed, chemical sediments. Other samples retain remnants of LREE depletion but are beginning to lose the distinct La, Eu and Y positive anomalies and are interpreted as metasomatised chemical sediments. Finally there are some siliceous samples with completely different trace element patterns that are interpreted as rocks of non-sedimentary origin, and include metasomatised mafic rocks. The positive La/La*$_{SN}$, Eu/Eu*$_{SN}$ and Y_{SN} anomalies found in Isua BIFs and other Eoarchaean Greenland samples, such as G91/26 from Akilia, suggests that the processes of carbonate ion complexation controlling the REE − Y patterns were already established in the hydrosphere at the start of the sedimentary record 3,600–3,850 Ma ago. This is in accord with the presence of Eoarchaean siderite-bearing marbles of sedimentary origin, and suggests that CO_2 may have been a significant greenhouse gas at that time.

Communicated by T.L. Grove.

C. R. L. Friend
45 Stanway Road, Risinghurst, Headington,
Oxford OX3 8HU, UK

A. P. Nutman
Chinese Academy of Geological Sciences,
Institute of Geology, 26 Baiwanzhuang Road,
Beijing 100037, China

A. P. Nutman
Department of Earth and Marine Sciences,
Australian National University,
Canberra, ACT 0200, Australia

V. C. Bennett (✉) · M. D. Norman
Research School of Earth Sciences,
Australian National University,
Canberra, ACT 0200, Australia
e-mail: vickie.bennett@anu.edu.au

Keywords Archaean · Greenland · Banded iron-formation · Chemical sediments · Seawater composition · Akilia

Introduction

Modern chemical sediments have characteristic geochemical signatures (e.g. Elderfield 1988; Sholkovitz et al. 1994; Nozaki et al. 1997) comprising shale normalised LREE depletion (here discussed relative to PAAS = Post Archaean Average Shale; Taylor and McLennan 1985) and positive La/La*, Eu/Eu* and Y anomalies (see Bolhar et al. 2004). For these studies, the standard REE plot has been modified to include Y between Dy and Ho (Bau and Dulski 1996), allowing immediate identification of those samples that have all these characteristics. This signature is most widely documented in sediments precipitated from seawater, but it has also been documented in fluvial, alkaline lake and groundwater systems (e.g. Cantrell and Byrne 1987; Johannesson and Lyons 1994; Johannesson et al. 1996, 2005, 2006). Therefore, in this paper we refer to this geochemical signature as "*seawater-like*". The origin of these distinctive REE − Y patterns is attributed to precipitation from circumneutral to high pH waters where solution complexation of the REEs was dominated by carbonate ions (e.g. Cantrell and Byrne 1987; Johannesson et al. 2005; Luo and Byrne 2004; Tang and Johannesson 2003; Sonke and Salters 2006).

Via chemical sediments of increasing age this REE + Y signature can be tracked back in time through the Phanerozoic into the early Precambrian, where it is characteristic of banded iron-formations (BIF), e.g. Derry and Jacobsen (1990), Alibert and McCulloch (1992), Bau (1993), Bau and Dulski (1996) and Bolhar et al. (2005). The international BIF reference material IF-G (Govindaraju 1995) was prepared from chemical sediments (e.g. Appel 1980; Dymek and Klein 1988) that are part of the amphibolite facies ≥3,700 Ma Isua supracrustal belt (Moorbath et al. 1973; Nutman et al. 1997a) of the Eoarchaean Itsaq Gneiss Complex, SW Greenland (Fig. 1a, b). IF-G has a trace element signature (Dulski 2001) similar to that of chemical sediments deposited from Phanerozoic seawater and is of undisputed sedimentary origin. Outside the Isua supracrustal belt, other units of SW Greenland Eoarchaean supracrustal material contain rocks also interpreted as chemical sediments (McGregor and Mason 1977; Nutman et al. 1996). However, these were metamorphosed to a higher grade than the Isua metasediments in the early Archaean, in some cases up to granulite facies (Griffin et al. 1980; Friend and Nutman 2005a), and were variably retrogressed (e.g. Friend and Nutman 2005b). Due to this polyphase recrystallisation and deformation there is essentially nothing left of their original sedimentary textures, requiring a stronger reliance on geochemistry to correctly identify their protoliths.

The purpose of this paper is to examine the extent of seawater-like signatures in the siliceous and calc-silicate rocks and marbles in the Eoarchaean Itsaq Gneiss Complex, and to monitor the effects of high-grade metamorphism and metasomatism upon those patterns. This study includes further results from the unit of siliceous and calc-silicate rocks from Akilia Island, which has been the focus of debate centered on whether it contains metasedimentary rocks (e.g. Fedo and Whitehouse 2002a vs. Dauphas et al. 2004), and chemical evidence of Eoarchaean life (e.g. Mojzsis et al. 1996 vs. Lepland et al. 2005). Correct identification of a seawater-like signature in Eoarchaean sediments (e.g. Bolhar et al. 2004, 2005) is of additional significance as evidence of complexation of REE via carbonate ions supports the possibility of Eoarchaean sedimentary carbonates, and furthermore suggests that CO_2 could have been a significant greenhouse gas in the early atmosphere.

Geology and sampling

The Eoarchaean rocks of the Nuuk district are known collectively as the Itsaq Gneiss Complex (summary in Nutman et al. 1996). The entire complex has been repeatedly metamorphosed to amphibolite facies and much of it is strongly deformed. At least 90% of the Complex is orthogneisses derived from tonalitic to granitic protoliths; the remaining 10% consists mainly of mafic inclusions within the orthogneisses. These mafic rocks are dominated by amphibolites derived from volcanic rocks associated with siliceous ± magnetite and calc-silicate rocks, which are accepted as, or are candidates for, chemical sediments. All of the possible chemical sedimentary rocks form less than 1% of the Complex.

The Complex occurs in two Neoarchaean tectonic blocks, the Isukasia and Færingehavn terranes (Friend and Nutman 2005b and Refs. therein). The Isukasia terrane contains the c. 35 km long *Isua supracrustal belt* (Fig. 1b) that is the largest body of volcano-sedimentary rocks in the Complex. U/Pb zircon dates of ≥3,795 and 3,710 Ma have been obtained for different volcanic units, indicating that the belt contains more than one Eoarchaean sequence (Nutman et al. 1996, 1997a, 2002a; Crowley 2003). The belt's northern edge is largely in tectonic contact with c. 3,700 Ma tonalitic gneisses (e.g. Nutman et al. 1997a, 2002a; Crowley et al. 2002), whilst sheets of c. 3,795 Ma tonalites, emanating from the southern gneisses, widely intrude amphibolites with rare relict pillow structures along its southern edge (e.g. Nutman et al. 1997a, 2002a;

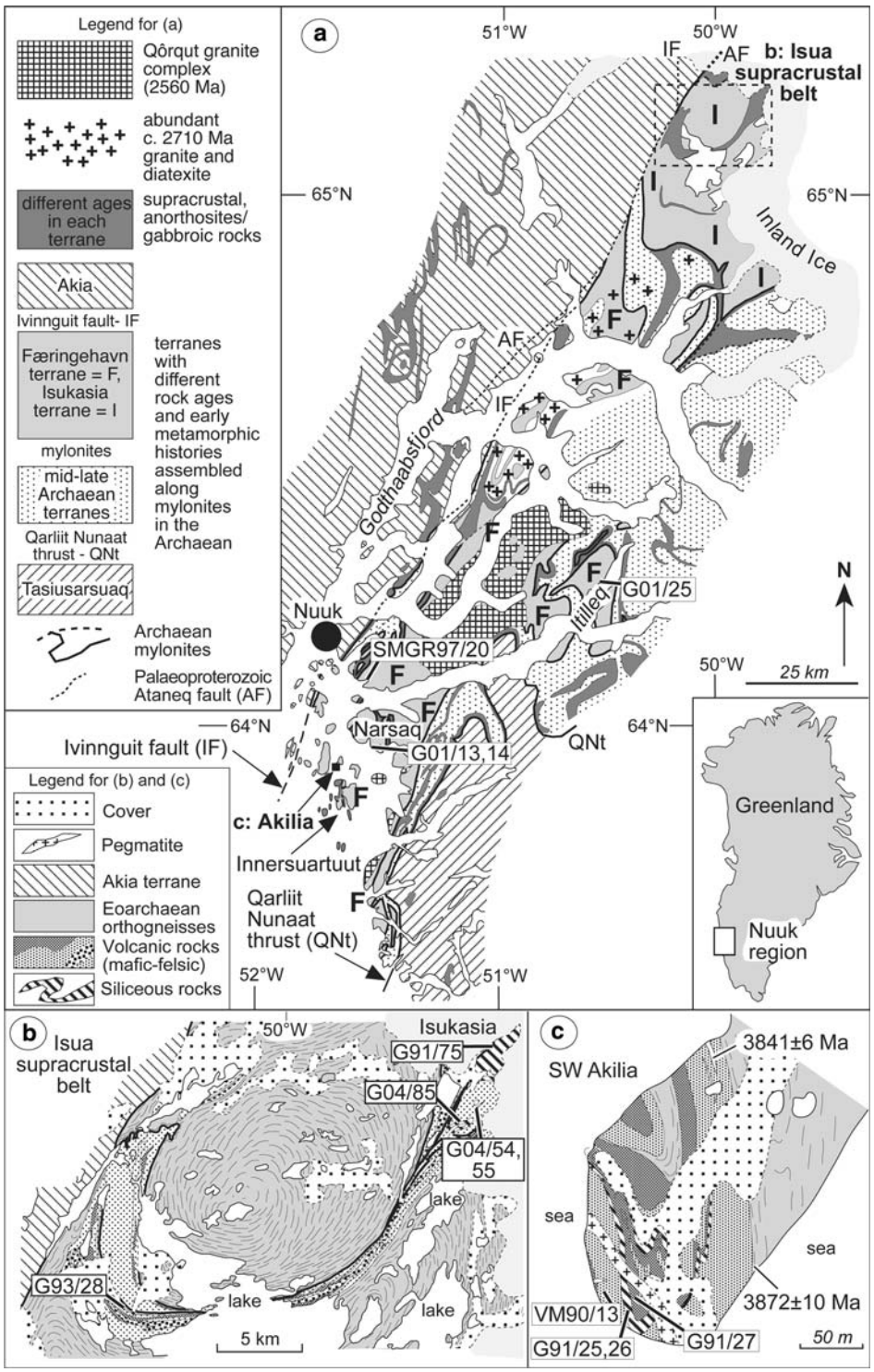

Fig. 1 **a** Location of discussed samples in the Itsaq Gneiss Complex, Nuuk region. *Inset* shows the position of the Nuuk region within the Archaean craton. **b** Detail of part of the Isukasia Terrane showing the Isua supracrustal belt (adapted from map in Nutman et al. 2002a), and the locations of the studied samples. **c** Detail of SW Akilia (island) in the Færingehavn Terrane south of Nuuk (adapted from map in Nutman et al. 2002b)

Crowley 2003). Although it is now accepted that the belt was partitioned by Eoarchaean tectonic breaks and comprises units of different ages, its exact architecture is still a subject of debate (e.g. Komiya et al. 1999; Myers 2001; Nutman et al. 2002a). The belt contains diverse quartz-rich rocks accepted as chemical sediments (e.g. Moorbath et al. 1973; Appel 1980; Dymek and Klein 1988), of which quartz + magnetite ± amphibole BIF is the most abundant. The prominent Isua BIF unit at the eastern end of the belt was first dated using whole-rock techniques and produced a Pb–Pb regression age of 3,710 ± 70 Ma (Moorbath et al. 1973; Moorbath and Whitehouse 1996).

A chert from the same unit has yielded an age of 3,691 ± 6 Ma from a few volcanogenic zircons recovered from it (Nutman et al. 2002a). Bolhar et al. (2004) demonstrated that some finely banded magnetite + quartz rocks as well as a carbonate + quartz + amphibole rock from the east of the belt display a seawater-like REE + Y signature. Thus the Isua BIF units are chemical sediments and as old as c. 3,700 Ma. Despite widespread evidence of carbonate metasomatism in the belt (Rose et al. 1996; Rosing et al. 1996), Bolhar et al. (2004) showed that with careful sample selection, subtle geochemical protolith signatures related to depositional environment are preserved in some of the Isua chemical sedimentary rocks. Geochemical data are reported here for a new Isua suite, representing most of the range of chemical sediments including a chert, two quartz + carbonate + amphibole rocks, one quartz + magnetite ± amphibole BIF and one quartz + carbonate + magnetite + amphibole BIF.

The Eoarchaean rocks south of Nuuk belong to the Færingehavn terrane (Fig. 1), from where McGregor and Mason (1977) described the "*Akilia association*" of supracrustal rocks that are mafic and siliceous enclaves within the orthogneisses. Zircon dating indicates that the supracrustal rocks in the Færingehavn terrane comprise units of different age (e.g. Nutman et al. 1996). Trace element signatures from BIF at two new localities, Narsaq and Itilleq (Fig. 1), are reported here. G01/13 (63°58.23′N 51°32.69′W) and G01/14 (63°58.22′N 51°32.68′W) are magnetite + quartz ± amphibole rocks within an enclave of mafic and siliceous rocks on the south coast of Narsaq. These are typical of the high-metamorphic grade (up to granulite facies) BIF enclaves scattered throughout the Itsaq Gneiss Complex south of Nuuk (McGregor and Mason 1977). The samples are layered on a millimeter scale, but due to the high strain and increase in grain size through metamorphic recrystallisation, this is a transposed structure, and no original sedimentary layering is preserved. G01/25 (64°17.21′N 50°31.06′W) is from a thoroughly recrystallised <1 m thick quartz + magnetite + pyroxene + amphibole ± garnet layer in a mafic and siliceous supracrustal enclave that crops out for c. 100 m on the northern shore of Itilleq (Fig. 1).

From a c. 5 m thick unit of siliceous rocks on southwest Akilia (Fig. 1c), G91/26R is an additional portion of the G91/26 layer used in earlier studies (Mojzsis et al. 1996; Nutman et al. 1997b; Friend et al. 2002), whereas G91/25 is an adjacent layer of finely banded quartz + pyroxene rock. Both of these samples are from layers that are finer grained than much of the more coarsely crystalline quartz + pyroxene + amphibole ± garnet siliceous unit present in this outcrop. The complexity and chemical heterogeneity of this siliceous unit was recognized in Nutman et al. (1997b), where it was described as ... "traversed and locally extensively infiltrated by quartz and pyroxene ± garnet ± amphibole veins. Such secondary material can form during diagenesis and then be metamorphosed, or might have developed during high-grade metamorphism. This veining and silica penetration is superimposed on top of the layering in the unit interpreted as a BIF." Thus G91/25, G91/26 and G91/26R were collected from the part of the siliceous unit with the finest grain size and thinnest layering, where the degree of metasomatic alteration was considered to be least but not necessarily entirely absent. Our criteria in selecting samples with the least metasomatic alteration was the finer grain size with magnetite-bearing layering and the absence of discordant coarse-grained quartz or calc-silicate veins.

The debate surrounding the interpretation of the Akilia siliceous unit and sample G91/26 has several strands. First, there are concerns whether G91/26 is the remnant of a water-lain chemical sediment (Nutman et al. 1997b; Friend et al. 2002; Dauphas et al. 2004), or whether the whole of the unit containing G91/26 is a metasomatically altered, silicified, ultramafic igneous rock (Myers and Crowley 2000; Fedo and Whitehouse 2002a, b; Bolhar et al. 2004). This has bearing on whether the protoliths of this unit were a potential habitat for early life. Second, a proposed age of ≥3,850 Ma (e.g. Nutman et al. 1996, 1997b, 2002b) for these Akilia rocks has been questioned. This zircon age comes from a discordant tonalite sheet (3,841 ± 6 Ma site on Fig. 1c) within the Akilia enclave, and has been confirmed using both ion probe depth profiling (Mojzsis and Harrison 2002) and single crystal ID-TIMS U-Pb dating (Krogh et al. 2002) on a tonalite from the same site. However, this sheet is disputed as being cross-cutting (Myers and Crowley 2000) and the age of the sheet has been argued to be c. 3,650 Ma with all of the old grains inherited (Whitehouse et al. 1999; Whitehouse and Kamber 2005). Debates over the age for this unit and evidence used for ancient life are continued elsewhere (most recently by Whitehouse and Kamber 2005; Friend and Nutman 2005a; Nutman and Friend 2006) and the focus in this paper is solely on whether the siliceous lithology represented by sample G91/26 was sedimentary or metasomatic in origin.

Analytical techniques

Samples were chipped using a hand press and then powdered in an alumina mill. Major elements were determined by XRF at Geoscience Australia. Trace elements were determined by ICPMS at the Australian National University using two independent methods: solution aspiration following acid digestion, and laser ablation of a glass prepared by fusing the sample with a Li-borate flux. The

primary motivation for the laser ablation analyses was to ensure that refractory phases such as zircons and chromites were digested completely by the Li-borate fusion. The solution aspiration analyses were similar to previously described procedures (Norman et al. 1998). A weighed ca. 0.1 g split of the sample powder was dissolved in distilled HF and HNO_3 acids in a screw-cap Teflon vial. The solution was brought to a final volume of 100 ml in 4% HNO_3, and 50 ppb Be, 10 ppb As, 5 ppb In, 5 ppm Re, and 5 ppb Bi added as internal standards. The solution was aspirated into an Agilent 7500 quadrupole ICP-MS using a glass concentric nebulizer and a double pass spray chamber that was temperature controlled to 1°C. Each analysis consisted of five scans of the mass range using a dwell time of 0.1 s per mass. BHVO-1 was used as the calibration standard for element sensitivities, using values of Eggins et al. (1997), except for Sr = 396 ppm, Zr = 175 ppm, Nb = 18.8 ppm, Y = 24.9 ppm and Er = 2.4 ppm (Norman et al. 2004). Corrections for instrumental drift were applied by normalising measured intensities of the internal standard elements to the BHVO-1 calibration solution. This was done by interpolating between internal standard masses assuming linear drift along the mass range, except for Li, which was normalised to Be, and Th and U, which were normalised to Bi. Procedural blanks were subtracted from the drift-corrected data. Reference materials BIR-1 (Icelandic basalt) and KIL93-1489 (Kilauea basalt; Eggins et al. 1997) were analysed in the same session with G91/26 (Table 1). For the laser ablation ICPMS analyses, 0.05 g of whole rock powder was fused with 0.15 g of a mixed Li-tetraborate/Li-metaborate flux in a graphite crucible at 1,000°C, followed by quenching in air (Norman et al. 1989, 2003, 2004; Odegard et al. 1998; Eggins 2003; Yu et al. 2003). The glass bead was mounted in epoxy and ablated under a mixed He + H atmosphere using an excimer 193 nm laser operated at 10 Hz and 100 mJ/pulse. A laser spot diameter of 70 microns was used and the sample was translated horizontally under the laser beam during the analysis. Data were collected in time-resolved mode with a dwell time of 0.02 s per mass. Backgrounds were collected on the carrier gas for 30 s prior to ablation and subtracted from the mean count rate measured on the sample. The NIST 612 glass was used to calibrate relative element sensitivities (Norman et al. 1998, 2004), and the data normalised to the CaO content of the bulk rock as determined by XRF. The major and trace element composition of G91/26, literature data for IF-G and data for other samples are given in Table 1. Two different samples G91/26 and G91/26R and two different crushes of G04/85 (Table 1) were used to evaluate sample homogeneity and repeat analyses were carried out on G04/54 and G04/55 as a demonstration of reproducibility. In addition, seven samples were analysed by both solution and laser methods (Table 1). There is very good agreement in the results from the two methods for most elements, including the REE, with variation between the two datasets, even for very low concentration samples (e.g. G91/75) typically less than 10% (Table 1) and producing parallel trace element patterns and similar element anomalies (Table 1; Fig. 2a). An exception is for Zr and Hf, where for four samples (G01/25, G04/55A, G04/85 and G91/75) the solution data yields significantly lower concentrations. This plausibly results from incomplete dissolution of very minor amounts of zircon or other zirconium phase during closed beaker dissolution as compared with fusion methods. Two different parts of sample G04/85, each about 1 kg, were powdered separately. The solution and laser data for the first split are in good agreement, but with the second rock split having overall higher trace element concentrations and similar Pr, but slightly lower Eu and higher La anomalies. This is interpreted as representing small-scale sample heterogeneity, even in this well-preserved quartz + magnetite BIF from the eastern Isua supracrustal belt, whose sedimentary pedigree is well established.

Results

Major elements

SiO_2 ranges from 54 to 97 wt% (Isua) and 60 to 83 wt% (south of Nuuk), whereas Fe_2O_3* (Fe_2O_3* = total Fe expressed as Fe_2O_3) ranges between 7 and 49 wt% (Isua) and 27 and 47 wt% (south of Nuuk; Table 1). These two oxides dominate the samples, and in the other major elements there is little evidence of any substantial terrigenous input. For example, no correlations between Al_2O_3, MgO and TiO_2 were found, and in all cases the abundance of TiO_2 is low. Isua samples G04/54 and G04/55 show higher CaO, reflecting their carbonate content. Compared to the international reference material BIF IF-G from Isua, Akilia sample G91/26 has roughly half the amount of iron and is more siliceous (ca. 62 vs. 41 wt%). Sample G91/25 is more calcic with lower iron content than G91/26 (Table 1). G91/26 has higher MgO (6.19 wt%) relative to IF-G (1.89 wt%), but within the range of compositions observed for Isua BIF (Dymek and Klein 1988). G91/26 and G91/25 are also more calcic than IF-G, reflected by abundant clinopyroxene and amphibole in their metamorphic assemblages. This probably reflects metamorphic decarbonation reactions between silica and carbonate of the sedimentary protolith (Nutman and Friend 2006). This is in accord with lower grade quartz + carbonate + amphibole Isua rocks with seawater-like REE + Y signatures (Bolhar et al. 2005) and our samples G04/54 and G04/55, which

Table 1 Major and trace element concentrations for chemical sediments from southwest Greenland

Sample	IF-G std	IF-G std	G91/26		G91/26R	G91/25 qtz-pyx		G01/13	G01/14	G01/25	
Ref.	1	2	Soln.	3	LA	LA	Soln.	LA	LA	LA	Soln.
Locality	Isua	Isua	Akilia		Akilia		Akilia	Narsaq	Narsaq	Ittilleq	
SiO_2 wt%	41.20		61.94		66.80	82.97		59.83	52.22	59.90	
TiO_2	0.01		0.04		0.01	0.01		0.02	0.15	0.20	
Al_2O_3	0.02		0.22		0.16	0.42		0.35	0.85	7.21	
Fe_2O_3*	55.85		26.91		27.55	11.60		40.14	46.65	26.14	
MnO	0.04		0.37		0.33	0.19		0.12	0.08	0.27	
MgO	1.89		6.19		5.06	3.27		2.63	2.86	2.81	
CaO	1.55		4.48		2.20	3.58		0.64	2.87	3.74	
Na_2O	0.03		ND		0.06	0.06		0.08	0.15	0.26	
K_2O	0.01		ND		0.01	0.01		0.01	0.04	0.16	
P_2O_5	0.06		0.02		0.04	0.02		0.03	0.05	0.10	
SO_3					1.36	0.38		0.02	0.26	4.80	
Total ppm	100.67		100.17		103.58	102.51		103.87	106.18	105.59	
Sc	0.3	0.294	0.6	1.5			1.7				4.3
Ti			14	15	10	17		60	825	1,164	
Cr	4	17	0.7	6	10	12		19	15	37	
Ni	23	24	187		172	59	60	28	33	223	207
Co	29.0		9.9		9.7	5.8	5.9	3.2	6.4	49.0	44.5
Ga	0.07		0.6		0.8	0.7	0.64	0.6	3.2	10.1	9.32
Rb	0.04	0.29	0.06	0.10	0.13	0.34	0.29	0.14	0.43	5.4	5.3
Sr	3	3.62	1.6	1.7	1.7	3.3	3.0	3.2	3.1	5.0	3.3
Ba	1.5	2.02	0.13	0.5	0.4	1.4	1.27	0.4	1.1	26.6	25.3
Y	9	9.17	1.2	1.1	1.2	2.9	2.8	3.8	11.6	19.2	18.1
Zr	1	0.560	0.67	0.9	0.9	3.1	1.8	2.1	3.9	57.0	45.4
Hf	0.04	0.018	0.014	0.017	0.019	0.105	0.075	0.070	0.208	1.54	ND
Nb	0.1	0.099	3.21	2.7	2.94	1.04	1.04	0.127	1.60	2.30	2.24
Ta	0.2		0.020	0.022	0.023	0.016	0.012	0.010	0.167	0.20	0.20
La	2.8	2.69	0.710		0.729	1.103	1.115	0.664	2.184	5.30	4.88
Ce	4	3.89	1.212	1.15	1.230	2.220	2.301	1.028	4.238	14.4	13.67
Pr	0.4	0.432	0.125	0.14	0.128	0.288	0.304	0.125	0.593	2.01	1.941
Nd	1.8	1.74	0.447		0.485	1.293	1.305	0.586	2.909	8.89	8.293
Sm	0.4	0.402	0.090	0.105	0.096	0.328	0.329	0.165	0.822	2.19	2.100
Eu	0.39	0.362	0.048	0.051	0.058	0.147	0.146	0.106	0.347	0.87	0.827
Gd	0.74	0.668	0.126	0.130	0.156	0.411	0.396	0.285	1.190	2.58	2.458
Tb		0.113		0.021	0.026	0.073	0.067	0.048	0.193	0.49	0.434
Dy	0.8	0.807	0.151	0.140	0.164	0.434	0.406	0.331	1.202	3.04	2.874
Ho	0.2	0.206	0.035	0.036	0.038	0.088	0.088	0.082	0.274	0.67	0.642
Er	0.63	0.623	0.090	0.091	0.115	0.258	0.231	0.277	0.807	2.07	1.817
Yb	0.6	0.578	0.099	0.098	0.122	0.208	0.208	0.232	0.653	1.97	1.846
Lu	0.09	0.093	0.016	0.016	0.020	0.032	0.031	0.040	0.100	0.31	0.283
Th	0.1	0.044	0.087	0.090	0.080	0.130	0.120	0.089	0.108	1.83	2.37
U	0.02	0.022	0.075	0.110	0.073	0.040	0.030	0.048	0.096	0.66	0.632
Y/Ho	45	44	35	31	33	33	32	47	42	29	28
Ce/Ce*	0.85	0.82	0.93		0.92	0.91	0.96	0.82	0.86	0.99	0.99
La/La*	2.47	1.59	1.15		1.29	1.35	1.12	2.16	1.91	0.88	0.75
Pr/Pr*	0.88	0.98	1.00		0.97	0.99	1.02	0.94	0.97	1.03	1.06
Eu/Eu*		3.46		2.18	2.41	1.92	1.98	2.43	1.77	1.71	1.74

Table 1 continued

Sample	G93/28	G04/54			G04/55A			G04/85		G04/85R	G91/75	
Ref. Locality	LA Isua	LA	LA-dup Isua	Soln.	LA	LA-dup Isua	Soln.	LA Isua	Soln.	LA Isua	LA Isua	Soln.
SiO_2 wt%	71.86	54.04			86.60	86.75		53.78		53.54	97.07	
TiO_2	0.01	0.07			0.01	0.01		0.01		0.01	0.00	
Al_2O_3	0.31	1.72			0.31	0.31		0.19		0.25	0.16	
Fe_2O_3*	12.42	12.35			6.92	6.92		46.10		49.08	2.62	
MnO	0.42	0.79			0.32	0.32		0.06		0.06	0.08	
MgO	3.08	7.16			2.29	2.28		2.63		2.39	0.67	
CaO	6.21	13.49			2.78	2.78		0.23		0.18	0.94	
Na_2O	0.03	0.03			0.01	0.02		0.07		0.07	0.01	
K_2O	0.04	0.53			0.01	0.01		0.01		0.01	0.00	
P_2O_5	0.02	0.01			0.01	0.01		0.05		0.05	0.01	
SO_3	0.06	0.01			0.08	0.08		0.01		0.00	0.01	
Total ppm	94.45	90.21			99.34	99.50		103.13		105.64	101.58	
Sc				1.8			0.2		0.1			0.1
Ti	50	391	389		34	34		11		18	12	
Cr	16	37	36		9	9		6		10	13	
Ni	43	23	21	20.6	21	21	21	18	18.1	29	8	2
Co	6.8	3.1	2.9	3.0	2.4	2.4	2.5	2.9	3.4	3.3	0.7	0.6
Ga	0.6	2.0	1.9	1.95	0.4	0.4	0.4	0.5	0.60	0.8	0.2	0.13
Rb	1.56	16.7	16.5	17.8	0.47	0.50	0.41	0.13	0.08	0.20	0.39	0.30
Sr	8.7	18.1	17.7	17.4	9.8	9.9	10.3	0.4	0.5	1.0	1.6	1.5
Ba	7.0	349	335	332	5.0	5.0	5.4	1.0	0.55	1.0	1.0	0.9
Y	4.6	3.1	3.2	3.0	2.4	2.4	2.4	3.2	2.9	6.3	0.9	0.81
Zr	2.2	13.5	13.5	12.1	2.0	2.0	1.2	0.6	0.25	1.1	0.5	0.21
Hf	0.059	0.412	0.406	0.330	0.046	0.051	0.029	0.016	0.007	0.027	0.024	0.006
Nb	0.078	0.458	0.457	0.400	0.073	0.069	0.051	0.087	0.120	0.234	0.027	0.011
Ta	0.007	0.028	0.031	0.023	0.006	0.006	0.004	0.003	0.004	0.004	0.006	0.002
La	2.167	2.041	1.959	1.984	0.517	0.512	0.595	1.959	2.044	1.272	0.461	0.305
Ce	3.314	3.111	3.017	3.235	0.736	0.739	0.789	3.026	3.687	1.994	0.610	0.562
Pr	0.362	0.351	0.335	0.359	0.087	0.083	0.093	0.305	0.368	0.241	0.063	0.064
Nd	1.513	1.378	1.365	1.411	0.395	0.388	0.435	1.231	1.422	1.087	0.251	0.256
Sm	0.335	0.307	0.292	0.302	0.108	0.113	0.122	0.242	0.285	0.299	0.066	0.053
Eu	0.261	0.263	0.254	ND	0.124	0.125	0.129	0.175	0.205	0.232	0.056	0.050
Gd	0.467	0.362	0.365	0.354	0.200	0.198	0.232	0.304	0.323	0.502	0.083	0.073
Tb	0.075	0.059	0.062	0.053	0.034	0.033	0.038	0.050	0.049	0.090	0.014	0.012
Dy	0.444	0.353	0.355	0.332	0.238	0.233	0.268	0.329	0.315	0.620	0.087	0.081
Ho	0.107	0.077	0.080	0.076	0.056	0.058	0.066	0.077	0.078	0.152	0.021	0.019
Er	0.323	0.230	0.223	0.209	0.174	0.175	0.189	0.263	0.228	0.509	0.059	0.056
Yb	0.265	0.211	0.209	0.198	0.150	0.154	0.170	0.305	0.281	0.519	0.060	0.049
Lu	0.043	0.033	0.033	0.031	0.023	0.023	0.028	0.053	0.048	0.088	0.008	0.007
Th	0.083	0.295	0.287	0.270	0.034	0.034	0.034	0.032	0.035	0.033	0.026	0.023
U	0.033	0.064	0.066	0.058	0.022	0.022	0.016	0.015	0.016	0.022	0.012	0.005
Y/Ho	43	41	40	39	43	41	37	42	37	41	40	42
Ce/Ce*	0.85	0.84	0.85	0.88	0.79	0.81	0.76	0.89	0.97	0.83	0.80	0.93
La/La*	1.68	1.40	1.54	1.35	2.19	2.54	2.65	1.65	1.30	1.89	1.83	1.22
Pr/Pr*	0.95	1.00	0.97	0.99	0.94	0.91	0.92	0.93	0.94	0.95	0.95	0.99

Table 1 continued

Sample	G93/28	G04/54			G04/55A			G04/85		G04/85R	G91/75	
Ref. Locality	LA Isua	LA	LA-dup Isua	Soln.	LA	LA-dup Isua	Soln.	LA Isua	Soln.	LA Isua	LA Isua	Soln.
Eu/Eu*	3.34	3.91	3.83		4.20	4.17	3.86	3.20	3.45	2.88	3.75	4.03

ND not determined

Major element data in by XRF. Trace element data by laser ablation ICP-MS (LA) or solution ICP-MS (soln.) as indicated. Dup = duplicate splits of same powder analysed separately. R = new powders prepared from different splits of the rock

1: Govindaraju (1995), 2: Bolhar et al. (2005), 3: Nutman et al. (1997a). Fe_2O_3* = total iron expressed as Fe_2O_3

Ce/Ce* and Pr/Pr* calculated using methods of Bau and Dulski (1996), where Ce/Ce* = Ce SN/(0.5 La + 0.5 Pr) SN; Pr/Pr* = Pr SN/(0.5 Ce + 0.5 Nd) SN; Eu/Eu* = Eu SN/(0.67 Sm + 0.33 Tb) SN, La/La* = Ln SN/(3 Pr − 2 Nd) SN

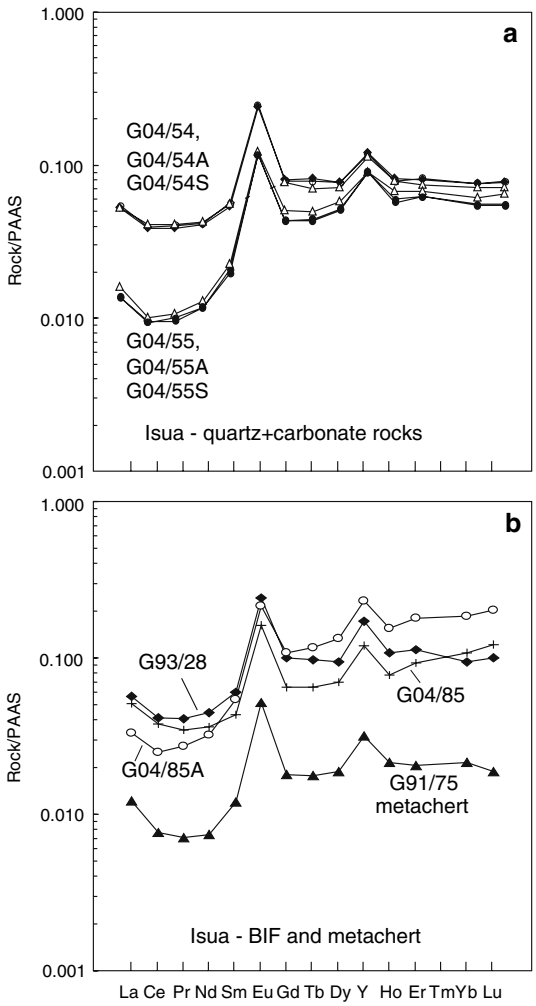

Fig. 2 PAAS normalised extended REE plots of Isua chemical sedimentary rocks. Duplicate analyses and comparison of results from both laser (A) and solution aspiration (S) methods are shown. **a** Quartz + carbonate + amphibole rocks. **b** BIF and chert samples. Results of two separate crushes of G04/85 are indicated

can be interpreted as silica + carbonate chemical sediments where decarbonation metamorphic reactions have not gone to completion.

The rare earth elements and yttrium

In all the samples analysed for this study the total abundances of REE are low. In Figs. 2, 3, 4 and 5, the new trace element data (Table 1) are compared with the compositions of other quartz-rich rocks from the region, and with data from Isua BIF (Dymek and Klein 1988; Bolhar et al. 2004). Normalisation to PAAS composition (Taylor and McLennan 1985) has been used to provide a common reference for sedimentary samples (e.g. Bau and Dulski 1996; Bolhar et al. 2004). Bau and Dulski (1996) discuss ambiguities in defining La and Ce anomalies and emphasise that comparison of sample variations must be based on the same mathematical formulation. La enrichment discussed here uses both Bau and Dulski's (1996) approach of calculating $Ce/Ce^* = Ce_{SN}/(0.5La + 0.5Pr)_{SN}$, where negative Ce/Ce*, particularly viewed in combination with Pr/Pr* is diagnostic of La enrichment, as well as the approach used by Bolhar et al. (2004) with $La/La^* = La_{SN}/(3Pr - 2Nd)_{SN}$. Eu and Pr anomalies (Table 1) are also calculated using the method of Bau and Dulski (1996) as $Eu/Eu^* = Eu_{SN}/(0.67Sm + 0.33 Tb)_{SN}$ and Pr/Pr^* as $Pr_{SN}/(0.5Ce + 0.5Nd)_{SN}$.

All of the Isua samples display the distinctive concave downwards, depletion of LREE (La to Nd) relative to the MREE and HREE on extended REE + Y patterns (Fig. 2). This pattern was considered by Bolhar et al. (2004) as being a seawater-like signature. Also present are the distinctive positive La anomalies (La/La* = 1.40–2.54), Eu (Eu/Eu* = 2.88–4.20) and Y (Y/Ho = 39.9–42.9) anomalies (Table 1, Fig. 2).

The analyses for the siliceous rocks from Narsaq and Itilleq (G01/13, G01/14, G01/25, Fig. 3) are compared to sample SMGR97/20 from Ugpik, which Bolhar et al. (2004) interpreted as a BIF with a seawater-like REE + Y signature preserved. The positive La anomaly is well developed in G01/13 and less so in G01/14, although the LREE depletion is less pronounced. Both samples have Eu and Y anomalies. The overall agreement between the patterns of G01/13 and SMGR97/20 is striking (Fig. 3). The REE + Y

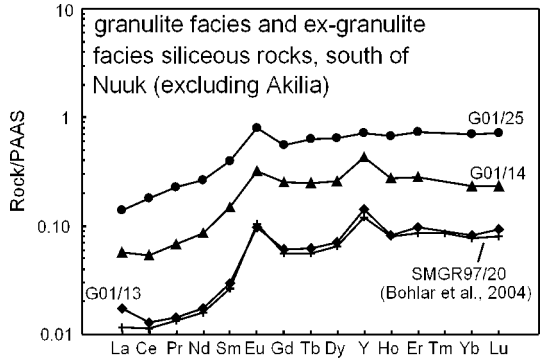

Fig. 3 PAAS normalized extended REE plots for magnetite-bearing siliceous rocks from diverse localities south of Nuuk. BIF sample SMGR97/20 from Ugpik (Bolhar et al. 2004) previously accepted as preserving a seawater signature, is plotted for comparison

pattern of the Itilleq sample G01/25 has no obvious concave downwards shape in the LREE pattern (La to Nd). Whilst there is a small positive Eu anomaly, that for Y is negligible. This is interpreted to suggest that a seawater-like signature is retained in G01/13, but in G01/14 the signature shows the commencement of corruption by metasomatic processes and that in G01/25 it is essentially gone.

For Akilia samples G91/26 and G91/26R the solution aspiration and laser ablation ICPMS trace element data sets agree well (Table 1). The PAAS normalised REE abundances of G91/26 with IF-G (Fig. 4a) and Isua BIF samples considered to represent seawater-derived chemical sediments at Isua (Fig. 2a, b), are all similar. They are characterised by very low absolute REE abundances, marked concave down depletions of the LREE and positive La, Eu and Y anomalies. G91/26 has both a positive La/La* anomaly (1.09–1.29) and a positive Eu/Eu* anomaly (2.04) relative to post-Archaean shales (Fig. 4b). In G91/26 the LREE are depleted (Pr/Yb_{SN} = 0.38) relative to both MREE and HREE, with MREE only slightly depleted relative to the HREE (Pr/Yb_{SN} = 0.34–0.46; Sm/Yb_{SN} = 0.40–0.54) well within the ranges described by Bolhar et al. (2004). G91/25 has essentially the same shape PAAS normalised pattern as G91/26, but at slightly higher overall abundance (Fig. 4b). The LREE are depleted relative to MREE and HREE (Pr/Yb_{SN} = 0.44; Sm/Yb_{SN} = 0.80) with a positive La/La* anomaly (1.35), but there appears to be the beginning of modification of the concave down shape, with Pr and Nd showing a smoother transition to Sm than in G91/26.

Other trace elements

Some other trace element abundances and ratios are also useful for discriminating between sediments deposited from seawater and those that are either modified or have suffered contamination with terrigenous material. Most samples including G91/25, G91/26 and G91/26R demonstrate low concentrations of lithophile elements normally associated with terrigenous sedimentary components, such as Zr (0.7 ppm), Th (0.09 ppm), Ga (0.6 ppm), and Ti (14 ppm). Ferromagnesian trace element concentrations are also low, e.g. Sc (0.06 ppm); V (3 ppm) and Cr (1 ppm) (Table 1). Abundances of Ni (190 ppm), Cu (460 ppm) and Zn (140 ppm) are somewhat elevated relative to average values for Isua BIF (c.f. Dymek and Klein 1988).

When plotting Zr versus Y/Ho (Fig. 5a), all samples with a seawater-like signature should plot at low Zr and with high Y/Ho ratios. Most of our samples fulfill this criterion, but some such as G04/54 from Isua have elevated Zr (using the laser ablation data). Samples IF-G and G91/26 plot within the seawater field with G91/26 very similar in composition to the average (n = 7) 3,450 Ma Warrawoona jasperites BIF of the Pilbara Craton (Y/Ho range = 26.3–43.5; Bolhar et al. 2005). In the Y versus Cr plot (Fig. 5b) all our samples have low Cr, with apart from two of them having Cr abundances less than IF-G. This again suggests low crustal contamination. Bau and Dulski (1996) use Ce/Ce* versus Pr/Pr* to define positive La anomalies, which they associate with a seawater-like signature. All of the new SW Greenland data plots within the positive La anomaly field (Fig. 5c).

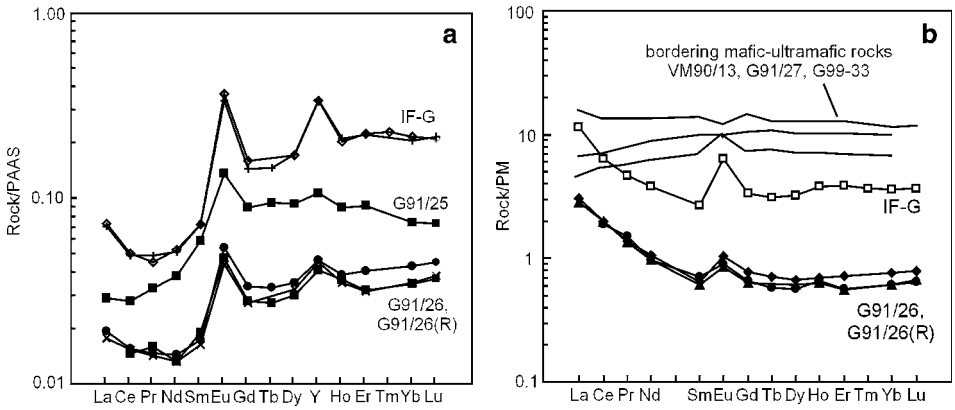

Fig. 4 Akilia samples. **a** Primitive mantle normalized REE data for G91/26 compared to the international BIF reference material IF-G, ultramafic rock G91/27 and amphibolite VM90/13. **b** PAAS normalized extended REE plots for IF-G and the Akilia siliceous samples G91/25, G91/26, and G91/26R

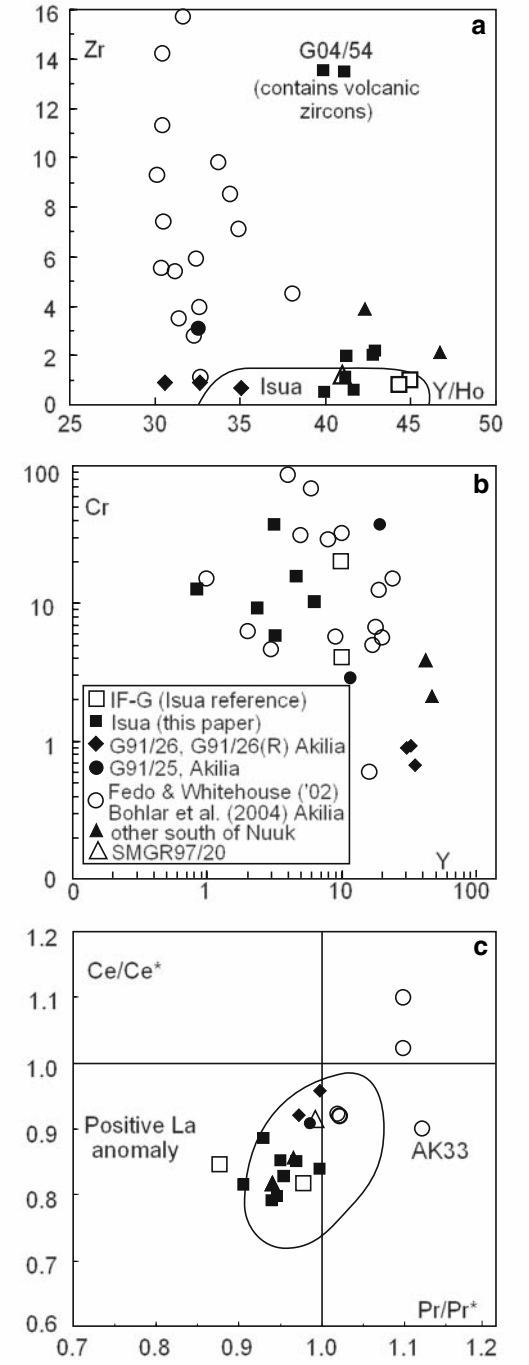

◀ **Fig. 5** Trace element and element ratio plots for the Isua rocks (*solid squares*), the international BIF reference material IF-G (*open squares*), G91/26 (*diamonds*), G91/25 (*dot*) and other BIF south of Nuuk (*triangles*). The data from Fedo and Whitehouse (2002a, b) and Bolhar et al. (2004) are plotted as *open symbols*. The *open triangle* is the BIF SMGR97/20 (Bolhar et al. 2004) from Ugpik. **a** Zr versus Y/Ho, the Isua field is for data in Bolhar et al. (2004). Apart from the high Zr carbonate-chert (G04/54) all plot at low Zr and high Y/Ho ratios. **b** Cr versus Y (as a measure of crustal contamination). **c** Ce/Ce* versus Pr/Pr*, where the anomalies are calculated following Bau and Dulski (1996) and with their field for BIF from the Penge and Kuruman formations shown. The Akilia siliceous rock data from Fedo and Whitehouse (2002a, b) largely plots off of the diagram

Discussion

Significance of marbles with seawater-like REE + Y signatures in the Isua supracrustal belt

Siderite- and ankerite-bearing marbles occur as volumetrically minor, laterally persistent layers between units of mafic volcanic rocks, ultramafic rocks and felsic schists in the Isua supracrustal belt (Nutman et al. 1984). Early geological and geochemical studies interpreted many of these marbles to have sedimentary carbonate protoliths, albeit it was always recognised that there had been considerable syn-kinematic mobility of carbonate with metasomatism during superimposed tectonothermal events (e.g. Nutman et al. 1984), particularly with carbonate being taken up by some of the ultramafic rocks (Dymek and Klein 1988). Other studies (Rose et al. 1996; Rosing et al. 1996) have suggested alternatively that all carbonate in the Isua supracrustal belt has emanated out of altered ultramafic rocks. In this latter interpretation, it has never been explained what was the ultimate source of the metasomatic carbonate, because clearly the carbonate does not belong to the original igneous assemblage of the ultramafic rock protoliths. The recognition of a seawater-like REE + Y signature in at least some Isua marbles (Bolhar et al. 2004, and this paper) strengthens the case that sedimentary carbonates are present in the Isua supracrustal belt, although by this we do not deny that now entirely metasomatic units can be present as well. The presence of these sedimentary carbonates has significance for early depositional environments, understanding the belt's tectonic evolution and placing constraints on Eoarchaean atmosphere composition.

Depositional environments

In the eastern part of the Isua supracrustal belt (Fig. 6), there is a multiply-folded package of amphibolites of "boninitic" composition (e.g. Polat et al. 2002, with rare relict pillow structures—Komiya et al. 1999) and amphibolites of differing compositions [also with rare relict pillow structures—Solvang (1999)—Fig. 7a], that are separated by a unit of mixed quartz + magnetite BIF (Fig. 7b) and chert + marble (Fig. 7c). The BIF is represented by sample G04/85 and the marbles by G04/54 and G04/55 (Fig. 1), all of which show seawater-like REE + Y signatures (Fig. 2).

Better preserved early Precambrian mixed BIF + chert + carbonate (siderite + ankerite) sedimentary packages, such as the Transvaal Supergroup of South

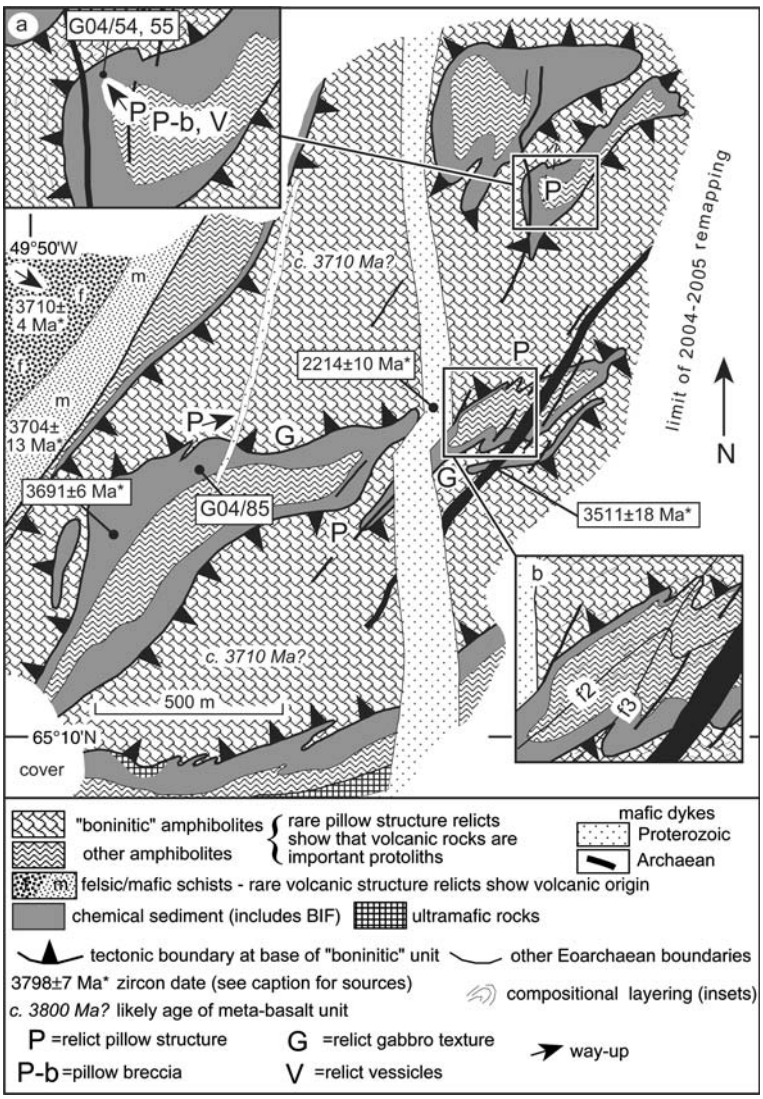

Fig. 6 Sketch map of part of the eastern Isua supracrustal belt

Africa, are usually interpreted as platformal sequences, formed in shallow to intermediate water depths (Klein and Beukes 1989). These carbonates might also form in shallow water in volcanic arc environments, and as such that they could occur in an oceanic environment, remote from continental crust. The presence of such carbonate-bearing sequences implies that some Isua sedimentary rocks were deposited in shallow to intermediate depositional depths, and not entirely all in deep-water environments. Evidence normally cited for a deep-water environment is the presence of possible turbiditic metasediments of volcanogenic provenance in the western part of the Isua supracrustal belt (Rosing 1999; Fedo et al. 2001). However, the presence of the sideritic carbonates interlayered with BIF indicating shallow to intermediate depositional depths, suggests that the sedimentary and volcanic rocks in the Isua supracrustal belt probably reflect a range of unrelated depositional environments, of different water depths.

Tectonic evolution of the Isua supracrustal belt

Carbonate sediment or marble units are ideal décollements in orogenic belts, permitting thrust sheets to glide with minimal friction over their footwall. A classic example of this in the European Alps, where basement nappes have ridden over thin carbonate and/or shale units (see Escher et al. 1993, for summary). Similar décollements along carbonate units with remnants of the mylonitic fabrics retained within included quartz-rich lithologies also occurs within the basement to the Caledonian orogen in North-East Greenland (e.g. Chadwick and Friend 1994). Such tectonic mechanisms have been proposed within Palaeoproterozoic Nagssugtoqidian orogen of West Greenland, where a footwall of Archaean orthogneisses is capped by a marble unit, over which lies an allochthonous sheet of juvenile Palaeoproterozoic arc plutonic and volcano-sedimentary rocks (Kalsbeek and Nutman 1996).

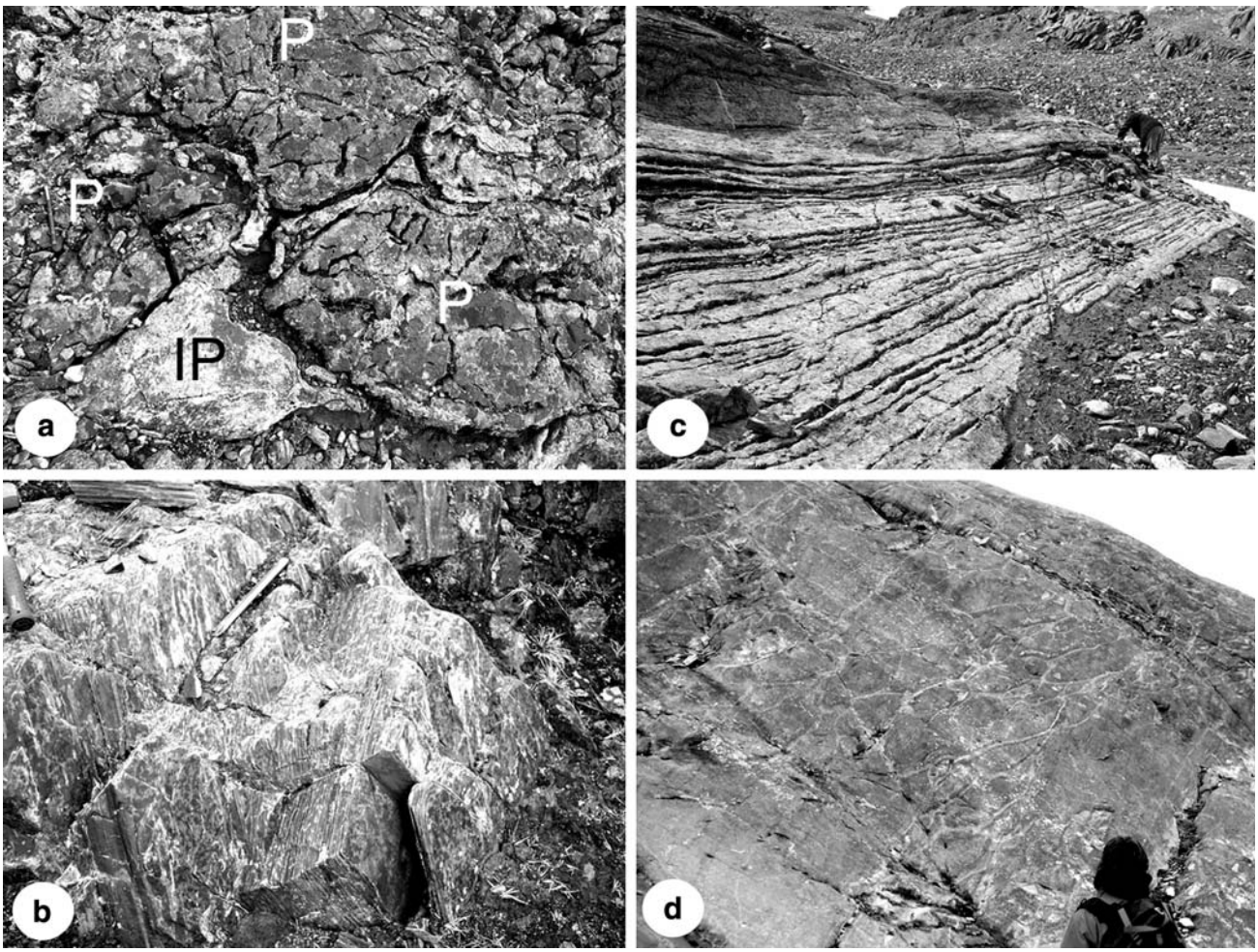

Fig. 7 *a* Pillows (*P*) preserved in mafic rocks, separated by siliceous inter-pillow material (*IP*). Locality of Solvang (1999), at 65°10.765′N 49°48.211′W. These pillows face up into the chemical sedimentary rocks shown in frames *b* and *c*. *b* Quartz + magnetite banded iron formation. Fine layering is transposed tectonic layering and does not represent fine-scale sedimentary layering. Sample G04/85 comes from the base of this outcrop at 65°10.310′N 49°49.224′W. *c* Deformed siliceous (metachert—*light grey*) with interlayers of carbonate + calcsilicate minerals (*dark grey*). Samples G04/54 and G04/55 were taken where the person is standing—65°10.760′N 49°48.153′W. *d* Pillows of "boninitic" affinity (see Polat et al. 2002), discovered by Komiya et al. (1999). Pillows (*dark grey*) are surrounded by siliceous inter-pillow material (*light grey*—65°10.375′N 49°49.365′W). This pillowed unit tectonically overlies the chemical sediment unit shown in frames *b* and *c*

The occurrence of marble units between metavolcanic rocks of different composition (and age?) in the Isua supracrustal belt indicates that such a tectonic process might have started by the Eoarchaean. Thus in the detailed map shown in Fig. 6, the relict pillow structures (Fig. 7a) first noted by Solvang (1999) face up into an overlying BIF + metachert + carbonate unit, for which samples G04/54 and G04/55 display seawater-like REE + Y signatures. The boundary between the pillowed amphibolites and the chert + marbles is heavily carbonated. Some of this alteration is early because ca. 3.5 Ga (amphibolite) Ameralik dykes cut through it, whereas there is also later alteration because the dykes are also cut by some carbonate + calcsilicate veins. The other contact of the BIF + metachert + marble unit is an early, pre-folding mylonite, on the other side of which are a distinct package of amphibolites with "boninitic" chemistry (Polat et al. 2002). Following this mylonite around the fold structures, it is found that the boninitic amphibolites locally preserve pillow structures close to the thrust (Figs. 6, 7d). The facing direction of these pillows is parallel to the folded mylonite (Fig. 6). Furthermore, along the same mylonite, the boninitic amphibolites also locally preserve relict gabbroic textures (Fig. 6). We interpret these rocks and structural information as follows: Structurally lowest in this part of the belt are a sequence of mafic to intermediate volcanic rocks (with the Solvang 1999, pillow locality), which was capped by a BIF + chert + carbonate sedimentary sequence. In this part of the belt, these sediments acted as a decollément, over which rode a thrust sheet of boninitic volcanic rocks

(Fig. 6). This thrust sheet is either internally composite or it cuts through the boninitic package at different levels, such that both pillow basalt and gabbroic rocks are truncated at the thrust (Fig. 6).

Composition of the Eoarchaean atmosphere

Siderite in Palaeoproterozoic carbonates is interpreted to indicate deposition from more acidic ocean waters than today, under an atmosphere with considerably high CO_2 content than the modern atmosphere (e.g. Ohmoto et al. 2004). This sedimentological evidence of high CO_2 content of the early atmosphere would indicate that CO_2 would be an important early greenhouse gas, warding off global glaciation under the early faint sun (e.g. Rye et al. 1995). Thus the presence of Precambrian sideritic limestone (or marble metamorphosed equivalent) is significant for understanding early atmosphere composition. The presence of sideritic protoliths for Eoarchaean marbles in the Isua supracrustal belt might extend such scenarios back to very early in Earth's history. This would be consistent with evidence for liquid water in the sedimentary record of Isua (Moorbath et al. 1973 onwards), and the seawater-like REE + Y signatures of some Isua marbles, showing complexing by carbonate ions was an important depositional mechanism.

Chemistry of the Akilia "early life" sample G91/26 and adjacent rocks

Chemical sedimentary origin for G91/26?

The controversial siliceous unit on Akilia also preserves rocks ("early life" sample G91/26 and G91/25) with the same REE patterns and anomalies as IF-G (Bau and Dulski 1996) and Isua BIF (Bolhar et al. 2004) (Fig. 4a,b) and therefore should also be interpreted as possessing a seawater-like signature. However, it should be pointed out that G91/26 is higher metamorphic grade rock that probably has nowhere entirely escaped metasomatism. We consider this an explanation that some of the distinctive elemental abundance anomalies have been reduced in size compared to those found in the better-preserved, lower metamorphic grade IF-G (Table 1). An extensive Fe isotope study that included G91/26 from Akilia and other samples from the nearby island Innersuartuut (Fig. 1a) revealed that these rocks are enriched in heavy Fe isotopes relative to a database of worldwide igneous rocks including adjacent amphibolite and ultramafic rocks on Akilia (Dauphas et al. 2004). This Fe isotopic variation is to the same extent as found in Isua BIF, further warranting the interpretation of G91/26 and related rocks from Akilia as originally derived from chemical sediments rather than being predominantly metasomatised mafic rocks. Therefore we contend that, *the actual portion* of the unit from which samples G91/25 and G91/26 were derived was of sedimentary origin. However, we have long recognised that there is a complexity to the Akilia siliceous unit (Nutman et al. 1997b), such that not all samples from it need be the same, and there is clearly metasomatism through the unit.

Origin of G91/26 by metasomatism of mafic rocks?

Fedo and Whitehouse (2002a, b) argued that the entire Akilia siliceous unit was derived by metasomatism (mostly silica addition) of adjacent mafic units. In terms of primitive mantle-normalised REE patterns (Fig. 4b) it is clear that G91/26 bears no relation to either the pattern or abundances of REE in the mafic units of igneous origin that bound the siliceous unit from which G91/26 was taken. Samples VM90/13 and G99/33 are amphibolites west of the siliceous unit and G91/27 is a hornblende-rich ultramafic rock to the east (Fig. 1c). Both meta-igneous rocks show a slight LREE depletion ($La/Yb_N = 0.67$), with a steady increase in abundance towards the MREE. If the Fedo and Whitehouse (2002a, b) hypothesis of silica enrichment of mafic rocks is correct, there should simply be a dilution of the relatively flat, slightly convex patterns obtained for these rocks (e.g. Friend et al. 2002), which there is not. There is no obvious mechanism for converting the flat REE patterns characteristic of igneous rocks in this area (Fig. 4a) into the bell-shaped pattern of G91/26.

Similarly, G91/26 lies at low Cr and high Y on a Cr versus Y plot (Fig. 5b) attesting to low mafic content even though it is adjacent to high-Cr mafic rocks. For G91/26 to be derived from the mafic units on either side would require a massive reduction of Cr, Ni, and Co which is incompatible with dilution of a mafic source material by SiO_2. Hence from simple mass balance arguments, increasing SiO_2 from 40 to 62 wt% will reduce Cr from 1,000 ppm to only 645 ppm. It is concluded that there is no geochemical similarity between G91/26 and the adjacent mafic and ultramafic rocks. This directly contradicts models that interpret G91/26 as not a metasediment (Bolhar et al. 2004) and lying within a unit of entirely metasomatised mafic igneous rocks (Fedo and Whitehouse 2002a, b).

Assessing terrigenous contamination

On the basis of our contention that G91/26 is derived from a chemical sediment, the extent of contamination upon deposition by terrigenous material is discussed here. A powerful tool in detecting terrigenous contamination is the

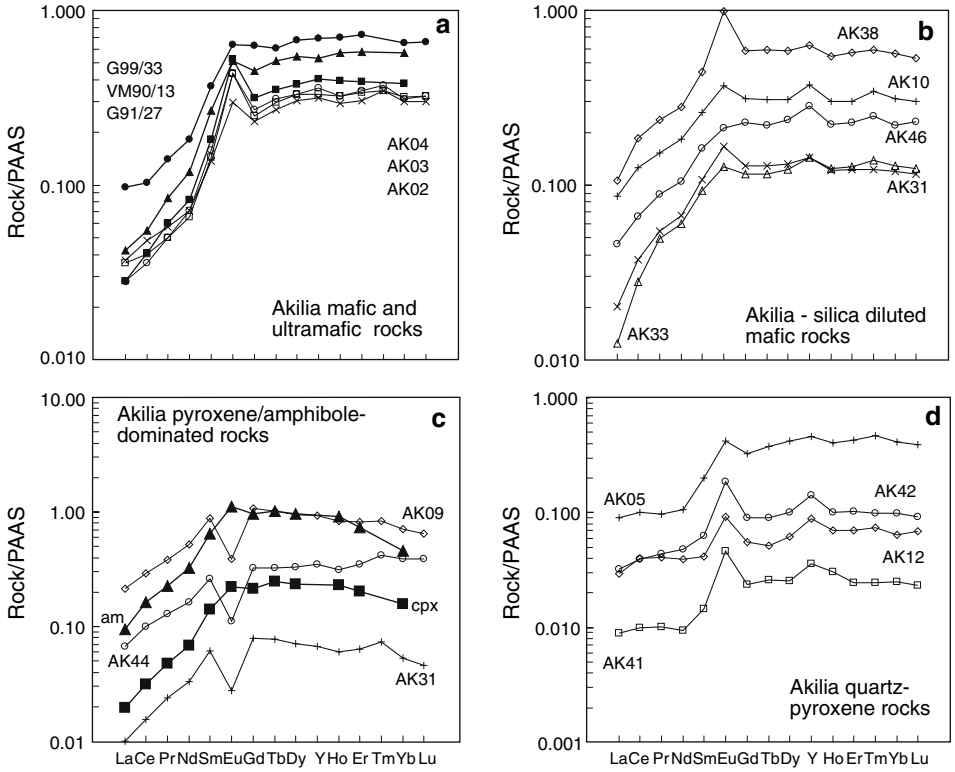

Fig. 8 Re-examination of Akilia siliceous rocks data from Fedo and Whitehouse (2002a) and Bolhar et al. (2004), all *open symbols*. **a** Ultramafic rocks with the addition of ultramafic rock G91/27 east of siliceous unit and amphibolites VM90/13 and G99/33 to the west (*solid symbols*). **b** Patterns that can be interpreted as proportions of mafic or ultramafic material (see **a**) diluted with quartz, and so consequently might be interpreted as metasomatised mafic igneous rocks. **c** Patterns that resemble those for pyroxene and/or amphibole (*solid symbols*). These can be interpreted as quartz pyroxene mixtures either as the result of metasomatism or metamorphic processes. **d** Samples that appear not to bear a relation to the types illustrated in **a**–**c** and might include some corrupted seawater signatures

Y/Ho ratio, because felsic crust has an essentially constant Y/Ho ratio of ~26 whereas seawater has a value of ~44 (Bolhar et al. 2004). G91/26 (Fig. 4b) has a Y/Ho ratio of 35.4, which falls within the lower end of the field of accepted Isua water-lain BIFs (Bolhar et al. 2004) but is well within the range observed for seawater-derived chemical sediments such as those from South Africa (Bau and Dulski (1996) and Western Australia (Bolhar et al. 2005).

Due to the much higher abundances of many lithophile elements (e.g. REE, Zr, Th) in terrigenous material, addition of only a few percent will mask the seawater-like trace element signatures of chemical sediments (Bolhar et al. 2004 and Refs. therein). Relatively insoluble and immobile lithophile elements such as Zr, Nb, and Ga may be used to detect crustal contamination (Bolhar et al. 2005), even in metamorphosed rocks. The low concentrations in G91/26 of the typically immobile crustally derived elements such as Zr (0.68 ppm), Hf (0.014 ppm), Ga (0.6 ppm) and Sc (0.6 ppm), as well as the depleted LREE point to only minimal crustal contamination. Any possible very small terrigenous input was probably not felsic in character, because no volcano-sedimentary zircons were recovered from G91/26 (the few zircons recovered grew during later metamorphism—Nutman et al. 1997b). This is in contrast to samples such as G04/54 from the Isua supracrustal belt, where anomalously high Zr abundance (14 ppm) is reflected by the recovery of a few tiny volcanogenic zircons, which yield the age of deposition of the sample (Nutman, unpublished SHRIMP U/Pb data). The preservation of positive (albeit reduced relative to IF-G) La/La*, Eu/Eu* and Y anomalies in G91/26 also points to minimal masking of a seawater-like signature via terrigenous material (Table 1).

Diverse origins of Akilia siliceous rocks

Fedo and Whitehouse (2002a, b) and Bolhar et al. (2004) presented trace element data for many samples from the Akilia siliceous unit. These are contrasted with the extended REE patterns for the Akilia mafic and ultramafic rocks that bound the siliceous unit to the northwest (Fig. 8a). These siliceous unit samples have been re-examined in the light of the new data presented in this paper. The extended REE patterns reveal several sets with different patterns (Fig. 8). All of the meta-igneous mafic and ultramafic samples show depleted LREE with smooth, linear increasing transitions from La to Sm and slightly convex MREE and HREE. In Fig. 8b some quartz-clinopyroxene mixture analyses from Fedo and Whitehouse (2002a) plus sample AK33 (Bolhar et al. 2004) are plotted. These show approximately parallel patterns, at overall abundances varying by an order of magnitude, and

resemble the patterns for accepted mafic and ultramafic rocks (Fig. 8a, b). These can be interpreted as mafic or ultramafic rocks to which varying proportions of quartz have been added. Other Bolhar et al. analyses (Fig. 8c) are compared here to amphiboles and clinopyroxenes from Akilia rocks (McGregor and Mason 1977). It is immediately apparent that apart from Eu, clinopyroxene-dominated boudins AK09 and AK44 have patterns like those of the Akilia amphibole and clinopyroxene, with variation in REE level ascribed to silica dilution. Fedo and Whitehouse (2002a) attribute the variable Eu/Eu* anomaly to metamorphic conditions fluctuating around the Eu(II)/Eu(III) valence boundary. However, this leaves a group in Fig. 6d that have yet different signatures to those in Fig. 8a–c. On the basis of comparison with "corrupted" chemical metasediment samples G01/14 and G01/25 (Fig. 3) and G91/25 (Fig. 4a), we interpret that these samples had sedimentary protoliths (probably mixtures of quartz and carbonate) that were metasomatically modified. Whilst retaining Eu and Y anomalies, they have lost their positive La anomaly, but still retain the characteristic pattern of depleted LREE relative to the MREE and HREE.

We contend that our new data can be used to explain the dichotomy of opinion that exists over the interpretation of the Akilia siliceous rocks. For some of the rocks an origin as mafic or ultramafic rocks with added quartz is supported (Fig. 8a, b). However, whether quartz was added by silicification of a flow top or bottom as seen in many Archaean volcanic units (e.g. Lowe and Byerly 1999), or by later metamorphic/metasomatic silica introduction is unknown. Granulite facies metamorphism can produce monomineralic pyroxene veins (McGregor and Friend 1997). Some discordant clinopyroxene ± amphibole veins are present in the Akilia siliceous rocks. Pyroxene ± amphibole domains formed during granulite facie metamorphism would have REE patterns that resemble pyroxene (Fig. 8c) and can readily be accepted as metamorphic or metasomatic rocks.

Therefore, the Akilia siliceous unit contains several different components: (a) remnants of chemical sediments that preserve a seawater-like REE + Y signature (notably G91/26—albeit distinctive anomalies are not as pronounced), (b) silicified mafic/ultramafic rocks, (c) rocks dominated by pyroxene which have formed either from metamorphic remobilization or metasomatic activity, and (d) some metasomatised rocks where vestiges of a seawater-like REE + Y signature are preserved. Thus the lithological complexity of the Akilia siliceous unit is in accord with the original appraisal as containing chemical sediment that was variably overprinted by metasomatic and/or metamorphic processes (Nutman et al. 1997b).

Corruption of the seawater-like REE + Y signature

Bolhar et al. (2004) concluded that only one of their samples (SMGR97/20 from Ugpik) from south of Nuuk had a seawater-like REE + Y signature prerequisite for a chemical sediment protolith. G01/13 from Narsaq is identical in its REE + Y pattern to SMGR97/20 from Ugpik (Fig. 3), which corroborates the field interpretations (McGregor and Mason 1977) that more Eoarchaean chemical sediments are present in the Itsaq Gneiss Complex south of Nuuk. These data also show that even with metamorphism up to granulite facies (and subsequently retrogression), rocks can locally retain seawater-like REE + Y signatures identical to the Isua BIF and quartz + carbonate rocks that were only metamorphosed to middle amphibolite facies (see also Bolhar et al. 2004).

However, all those who have studied complex outcrops of Eoarchaean siliceous rocks like those on Akilia concur that they have been variably metasomatised, with at the very least addition of simple silica veins (Nutman et al. 1997b; Bolhar et al. 2004). Other metasomatic processes also have been involved, because some discordant veins consist entirely of clinopyroxene and amphibole, whereas others can carry garnet (Nutman et al. 1997b; Nutman and Friend 2006). These veins by the nature of their mineralogy are able to produce more complex chemical variation than simple silica addition, and have a greater potential to mask subtle compositional traits of the protolith rocks. With repeated strong deformation and high-grade metamorphism, metasomatic veins can be transformed into a banding that obscures and even obliterates any original depositional layering. We contend that in the suite of iron-rich siliceous rocks from south of Nuuk (Bolhar et al. 2004, and this paper), there is a compositional spectrum from slightly metasomatised chemical metasediments with corrupted seawater-like REE + Y signatures to strongly metasomatised rocks where this signature is so strongly modified that subtle trace element anomalies have been erased. Thus the pattern for Akilia quartz + pyroxene + amphibole rock G91/25 shows a slightly corrupted seawater-like REE + Y signature, and it can be explained as an extensively decarbonated version of quartz + carbonate + amphibole (meta)sedimentary rocks found in the lower grade Isua supracrustal belt (e.g. G04/55). Also samples G01/14 and G01/25 show increasingly corrupted seawater-like signatures. Given the high degree of strain and modification of these rocks, it is not known to what extent the superimposed granulite facies metamorphism per se is responsible for this modification, and to what extent the more complex tectonothermal history of these rocks makes it harder to select samples free from (early) metasomatic veining.

Conclusions

1. Depleted LREE, with positive La, Eu and Y in REE + Y (shale normalised) patterns interpreted as a seawater-like signature in unquestioned Isua Eoarchaean chemical sediments (e.g. Bolhar et al. 2004) have been used here as a template to show that other Eoarchaean siliceous rocks from SW Greenland were formed by a similar mechanism.
2. This study increases the stock of Isua supracrustal belt carbonate ± quartz ± calc-silicate rocks with identified seawater-like REE + Y signatures preserved, and thus their protoliths were probably chemical sediments. This follows earlier suggestions (e.g. Dymek and Klein 1988) that the belt contains chemical sedimentary carbonate units, albeit it has long been recognised that, as is the general case in high-grade metamorphic complexes, carbonate has been mobile and has metasomatised adjacent rocks (Nutman et al. 1984; Rose et al. 1996; Rosing et al. 1996).
3. The presence of carbonate sediments in the Isua supracrustal belt shows that some of its rocks were deposited in shallow water, as has been noted for better-preserved early Precambrian mixed BIF-carbonate-chert sequences (e.g. Klein and Beukes 1989). Furthermore, such carbonate-bearing units could act as decollements for the structural juxtaposition of mafic volcanic rocks of different age and chemistry found juxtaposed in the Isua supracrustal belt (e.g. Nutman et al. 2002a; Polat and Hoffman 2003).
4. Even with metamorphism up to granulite facies (and subsequent retrogression), siliceous rocks from south of Nuuk can locally retain geochemical signatures identical to the Isua BIF and quartz + carbonate rocks that were only metamorphosed to middle amphibolite facies (see also Bolhar et al. 2004).
5. The REE + Y pattern of Akilia sample G91/26, taken together with Fe isotope data (Dauphas et al. 2004), and U/Pb zircon geochronology indicating that these rocks are >3,850 Ma (Nutman et al. 1997a, 2000, 2002a; Mojzsis and Harrison 2002; Krogh et al. 2002), justify its interpretation as the oldest chemical sediment currently known (Nutman et al. 1997a; Friend et al. 2002). This conclusion contrasts with Fedo and Whitehouse (2002a, b) who contend that the chemical data for the G91/26 unit are more similar to those of meta-igneous rocks, with no parts of it showing chemical signatures resembling Isua chemical sediments (Bolhar et al. 2004). By re-evaluation of the data from Fedo and Whitehouse (2002a) and Bolhar et al. (2004), the Akilia siliceous unit is demonstrated to contain rocks derived from both chemical sediments (variably metasomatised) and metasomatised igneous rocks. A similar variation in chemistry can be found in the BIF unit at Narsaq (well-preserved G01/13 and corrupted G01/14) and so is not unique to Akilia.

Acknowledgments CRLF was funded through NERC grant NER/A/S/1999/00024; APN and VCB through ARC grant DP0342794. APN thanks Richard Arculus for giving him an honorary fellowship at the Department of Earth and Marine Sciences. Ross Taylor is thanked for comments on this manuscript. Ole Christiansen of Nunaminerals A/S is thanked for some logistic support in the field. The manuscript was greatly improved by the comments from the reviewers Karen Johannesson and B. Kamber.

References

Alibert C, McCulloch MT (1992) Rare earth element and neodymium isotopic compositions of the in banded iron-formations and associated shales from Hamersley, Western Australia. Geochim Cosmochim Acta 57:187–204

Appel PWU (1980) On the early Archaean Isua iron-formation, West Greenland. Precambrian Res 11:73–87

Bau M (1993) Effects on syn- and post-depositional processes on rare-earth element distribution in Precambrian iron formations. Eur J Mineral 5:257–267

Bau M, Dulski P (1996) Distribution of Y and rare-earth elements in the Penge and Kuruman iron formations, Transvaal Supergroup, South Africa. Precambrian Res 79:37–55

Bolhar R, Kamber BS, Moorbath S, Fedo CM, Whitehouse MJ (2004) Characterisation of early Archaean chemical sediments by trace element signatures. Earth Planet Sci Lett 222:43–60

Bolhar R, van Kranendonk MJ, Kamber BS (2005) A trace element study of siderite-jasper banded iron formation in the 3.45 Ga Warrawoona Group, Pilbara Craton—formation from hydrothermal fluids and shallow water. Precambrian Res 137:93–114

Cantrell KJ, Byrne RH (1987) Rare earth element complexation by carbonate and oxalate ions. Geochim Cosmochim Acta 51:597–605

Chadwick B, Friend CRL (1994) Reaction of Precambrian high-grade gneisses to mid-crustal ductile dreformation in western Dove Bugt, North-East Greenland. Rapp Grønlands Geløgiske Undersøgelse 162:53–70

Crowley JL (2003) U-Pb geochronology of 3810–3630 Ma granitoid rocks south of the Isua greenstone belt, southern West Greenland. Precambrian Res 126:235–257

Crowley JL, Myers JS, Dunning GR (2002) Timing and nature of multiple 3700–3600 Ma tectonic events in intrusive rocks north of the Isua greenstone belt, southern West Greenland. Bull Geol Soc Am 114:1311–1325

Dauphas N, Van Zuilen M, Wadhwa M, Davis AM, Marty B, Janney PE (2004) Clues from Fe isotope variations on the origin of early Archean BIFs from Greenland. Science 306:2077–2080

Derry LA, Jacobsen SB (1990) The chemical evolution of Precambrian seawater: evidence from REEs in banded iron formations. Geochim Cosmochim Acta 54:2965–2977

Dulski P (2001) Reference materials for geochemical studies: new analytical data by ICP-MS and critical discussion of reference values. Geostand Newsl 25:87–125

Dymek RF, Klein C (1988) Chemistry, petrology and origin of banded iron-formation lithologies from the 3800 Ma Isua supracrustal belt, West Greenland. Precambrian Res 37:247–302

Eggins SM (2003) Laser ablation ICP-MS analysis of geological materials prepared as lithium borate glasses. Geostand Newsl 27:147–162

Eggins SM, Woodhead JD, Kinsley L, Mortimer G, Sylvester PJ, McCulloch MT, Hergt JM, Handler M (1997) A simple method for the simultaneous and precise analysis of 40 or more trace elements in geological samples by ICP-MS using enriched isotope internal standardization. Chem Geol 134:311–326

Elderfield H (1988) The oceanic chemistry of the rare-earth elements. Philos Trans R Soc Lond A325:105–126

Escher A, Masson H, Steck A (1993) Nappe geometry in the Western Swiss Alps. J Struct Geol 15:501–509

Fedo CM, Myers JS, Appel PWU (2001) Depositional setting and paleogeographic implications of Earth's oldest supracrustal rocks, the >3.7 Ga Isua Greenstone Belt, West Greenland. Sediment Geol 141–142:61–77

Fedo CM, Whitehouse MJ (2002a) Metasomatic origin of quartzpyroxene rock, Akilia, Greenland, and implications for Earth's earliest life. Science 296:1448–1452

Fedo CM, Whitehouse MJ (2002b) Origin and significance of Archaean quartzose rocks at Akilia, Greenland. Science 298:917a

Friend CRL, Nutman AP (2005a) Complex 3660–3500 Ma orogenic episodes superimposed on juvenile crust accreted between 3850–3690 Ma: Itsaq Gneiss Complex, southern West Greenland. J Geol 113:375–397

Friend CRL, Nutman AP (2005b) New pieces to the Archaean terrane jigsaw puzzle in the Nuuk region, southern West Greenland: steps in transforming a simple insight into a complex regional tectonothermal model. J Geol Soc Lond 162:147–162

Friend CRL, Nutman AP, Bennett VC (2002) Origin and significance of Archaean quartzose rocks at Akilia, Greenland. Science 298:917a

Govindaraju K (1995) Update (1984–1995) on two GIT-IWG geochemical reference samples: albite from Italy, AL-1 and iron formation sample from Greenland, IF-G. Geostand Newsl 19:55–95

Griffin WL, McGregor VR, Nutman AP, Taylor PN, Bridgwater D (1980) Early Archaean granulite-facies metamorphism south of Ameralik, West Greenland. Earth Planet Sci Lett 50:59–74

Johannesson KH, Lyons WB (1994) The rare earth element geochemistry of Mono Lake water and the importance of carbonate complexing. Limnol Oceanogr 39:1141–1154

Johannesson KH, Stetzenbach KJ, Hodge VF, Lyons WB (1996) Rare earth element complexation behavior in circumneutral pH groundwaters: assessing the role of carbonate and phosphate ions. Earth Planet Sci Lett 139:305–319

Johannesson KH, Cortés A, Ramos Leal JA, Ramírez AG, Durazo J (2005) Geochemistry of rare earth elements in groundwaters from a rhyolite aquifer, central México. In: Johannesson KH (eds) Rare earth elements in groundwater flow systems. Springer, Dordrecht, pp 187–222

Johannesson KH, Hawkins DL, Cortés A (2006) Do Archean chemical sediments record ancient seawater rare earth element patterns? Geochim Cosmochim Acta 70:871–890

Kalsbeek F, Nutman AP (1996) Anatomy of the Early Proterozoic Nagssugtoqidian orogen, West Greenland, explored by reconnaissance SHRIMP U-Pb zircon dating. Geology 24:515–518

Klein C, Beukes NJ (1989) Geochemistry and sedimentology of a facies transition from limestone to iron formation deposition in the early Proterozoic Transvaal Supergroup, South Africa. Econ Geol 84:1733–1774

Komiya T, Maruyama S, Masuda T, Appel PWU, Nohda S (1999) The 3.8–3.7 Ga plate tectonics on the Earth; field evidence from the Isua accretionary complex, West Greenland. J Geol 107:515–554

Krogh TE, Kamo SL, Kwok YY (2002) An isotope dilution etch abrasion solution to the Akilia island U-Pb age controversy. Goldschmidt Abstracts (2002) A419

Lepland A, van Zuilen MA, Arrhenius G, Whitehouse MJ, Fedo C (2005) Questioning the evidence for Earth's earliest life—Akilia revisited. Geology 33:77–99

Lowe DR, Byerly GR (1999) Geologic evolution of the Barberton Greenstone Belt, South Africa. Geol Soc Am Sp Paper 329:319pp

Luo YR, Byrne RH (2004) Carbonate complexation of yttrium and the rare earth elements in natural waters. Geochim Cosmochim Acta 68:691–699

McGregor VR, Friend CRL (1997) Field recognition of rocks totally retrogressed from granulite facies: an example from Archaean rocks in the Paamiut region, South-West Greenland. Precambrian Res 86:59–70

McGregor VR, Mason B (1977) Petrogenesis and geochemistry of metabasaltic and metasedimentary enclaves in the Amîtsoq gneisses, West Greenland. Am Mineral 62:887–904

Moorbath S, O'Nions RK, Pankhurst RJ (1973) Early Archaean age for the Isua iron-formation, West Greenland. Nature 245:138–139

Mojzsis SJ, Harrison TM (2002) Establishment of a 3.8 Ga magmatic age for the Akilia tonalite (southern West Greenland). Earth Planet Sci Lett 202:563–576

Mojzsis SJ, Arrhenius G, McKeegan KD, Harrison TM, Nutman AP, Friend CRL (1996) Evidence for life on Earth before 3800 million years age. Nature 384:55–59

Moorbath S, Whitehouse MJ (1996) Age of the Isua supracrustal sequence of West Greenland. In: Chela-Flores J, Raulin F (eds) Chemical evolution: physics of the origin and evolution of life. Kluwer, Dordrecht, pp 87–95

Myers JS (2001) Protoliths of the 3.7–3.8 Ga Isua greenstone belt, West Greenland. Precambrian Res 105:129–141

Myers JS, Crowley JL (2000) Vestiges of life in the oldest Greenland rocks? A review of early Archaean geology in the Godthaabsfjord region, and reappraisal of field evidence for >3850 Ma life on Akilia. Precambrian Res 103:101–124

Norman MD, Leeman WP, Blanchard DP, Fitton JG, James D (1989) A comparison of major and trace elements by ICP, XRF, INAA, and ID methods. Geostand Newsl 13:283–290

Norman MD, Griffin WL, Pearson NJ, Garcia MO, O'Reilly SY (1998) Quantitative analysis of trace element abundances in glasses and minerals: a comparison of laser ablation ICPMS, solution ICPMS, proton microprobe, and electron microprobe data. J Anal Atomic Spectrosc 13:477–482

Nozaki Y, Zhang YS, Amakawa H (1997) The fractionation between Y and Ho in the marine enviroment. Earth Planet Sci Lett 148:329–340

Norman M, Robinson P, Clark D (2003) Major and trace element analysis of sulphide ores by laser ablation ICPMS, solution ICPMS, and XRF. Can Mineral 41:293–305

Norman MD, Garcia MO, Bennett VC (2004) Rhenium and chalcophile elements in basaltic glasses from Ko'olau and Molokai volcanoes: magmatic outgassing and composition of the Hawaiian plume. Geochim Cosmichim Acta 68:3761–3777

Nutman AP, Friend CRL (2006) Petrography and geochemistry of apatites in banded iron formation, Akilia, W. Greenland: consequences for early life. Precambrian Res 147:100–106

Nutman AP, Allaart JH, Bridgwater D, Dimroth E, Rosing MT (1984) Stratigraphic and geochemical evidence for the depositional environment of the early Archaean Isua supracrustal belt, southern West Greenland. Precambrian Res 25:365–396

Nutman AP, McGregor VR, Friend CRL, Bennett VC, Kinny PD (1996) The Itsaq gneiss complex of southern West Greenland: the world's most extensive record of early crustal evolution (3900–3600 Ma), Precambrian Res 78:1–39

Nutman AP, Bennett VC, Friend CRL, Rosing MT (1997a) ~3710 and >3790 Ma volcanic sequences in the Isua (Greenland)

supracrustal belt: structural and Nd isotope implications. Chem Geol 141:271–287

Nutman AP, Mojzsis SJ, Friend CRL (1997b) Recognition of >3850 Ma water-lain sediments in West Greenland and their significance for the early Archaean Earth. Geochim Cosmochim Acta 61:2475–2484

Nutman AP, Friend CRL, Bennett VC, McGregor VR (2000) The Early Archean Itsaq Gneiss Complex of southern West Greenland: the importance of field observations in interpreting age and isotopic constraints for early terrestrial evolution. Geochim Cosmochim Acta 64:3035–3060

Nutman AP, Friend CRL, Bennett, VC (2002a) Evidence for 3650–3600 Ma assembly of the northern end of the Itsaq Gneiss Complex, Greenland: implication for early Archean tectonics. Tectonics 21. doi:10.1029/2000TC001203

Nutman AP, McGregor VR, Shrashi K, Friend CRL, Bennett VC, Kinny PD (2002b) ≥3850 Ma BIF and mafic inclusions in the early Archaean Itsaq Gneiss Complex migmatites around Akilia, southern West Greenland? The difficulties of precise dating of zircon-free protoliths in migmatites. Precambrian Res 117:185–224

Odegard M, Dundas SH, Flem B, Grimstvedt A (1998) Application of a double-focusing magnetic sector inductively coupled plasma mass spectrometer with laser ablation for the bulk analysis of rare earth elements in rocks fused with Li2B4O7. Fresenius J Anal Chem 362:477–482

Ohmoto H, Watanabe Y, Kumazawa K (2004) Evidence from massive siderite beds for a CO_2-rich atmosphere before ~1.8 billion years ago. Nature 429:395–400

Polat A, Hofmann AW (2003) Alteration and geochemical patterns in the 3.7–3.8 Ga Isua greenstone belt, West Greenland. Precambrian Res 126:197–218

Polat A, Hofmann AW, Rosing MT (2002) Boninite-like volcanic rocks in the 3.7–3.8 Ga Isua greenstone belt, West Greenland: geochemical evidence for intra-oceanic subduction zone processes in the early Earth. Chem Geol 184:231–254

Rose NM, Rosing MT, Bridgwater D (1996) The origin of metacarbonate rocks in the Archaean Isua supracrustal belt. Am J Sci 296:1004–1044

Rosing MT, Rose NM, Bridgwater D, Thomsen HS (1996) Earliest part of Earth's stratigraphic record: a reappraisal of the >3.7 Ga Isua (Greenland) supracrustal sequence. Geology 24:43–46

Rosing MT (1999) 13C-depleted carbon microparticles in >3700 Ma sea-floor sedimentary rocks from West Greenland. Science 283:674–676

Rye R, Kuo PH, Holland HD (1995) Atmospheric carbon dioxide concentrations before 2.2 billion years ago. Nature 378:603–605

Sholkovitz ER, Landing WM, Lewis BL (1994) Ocean particle chemistry: the fractionation of rare earth elements between suspended particles and seawater. Geochim Cosmochim Acta 58:1567–1579

Solvang M (1999) An investigation of metavolcanic rocks from the eastern part of the Isua greenstone belt, West Greenland. Geological Survey of Denmark and Greenland (GEUS) Internal Report, Copenhagen, Denmark, 62 p

Sonke JE, Salters VJM (2006) Lanthanide-humic substances complexation. I. Experimental evidence for a lanthanide contraction effect. Geochim Cosmochim Acta 70:1495–1506

Tang J, Johannesson KH (2003) Speciation of rare earth elements in natural terrestrial waters: assessing the role of dissolved organic matter from the modeling approach. Geochim Cosmochim Acta 67:2321–2339

Taylor SR, McLennan SM (1985) The continental crust: its composition and its evolution. Blackwell, Oxford, 312 pp

Whitehouse MJ, Kamber BS (2005) Assigning dates to thin gneissic veins in high-grade metamorphic terranes: a cautionary tale from Akilia, southwest Greenland. J Petrol 46:291–318

Whitehouse MJ, Kamber BS, Moorbath S (1999) Age significance of U–Th–Pb zircon data from early Archaean rocks of West Greenland a reassessment based on combined ion-microprobe and imaging studies. Chem Geol 160:201–224

Yu Z, Norman MD, Robinson P (2003) Major and trace element analysis of silicate rocks by XRF and laser ablation ICPMS using lithium borate fused glasses: matrix effects, instrument response, and results for international reference materials. Geostand Newsl 27:67–89